VIP Surface Chemistry Very Important Paper

Deutsche Ausgabe: DOI: 10.1002/ange.201507631
Internationale Ausgabe: DOI: 10.1002/anie.201507631

First Principles Calculations for Hydrogenation of Acrolein on Pd and Pt: Chemoselectivity Depends on Steric Effects on the Surface

*Sakari Tuokko, Petri M. Pihko, and Karoliina Honkala**

Abstract: *The chemoselective hydrogenation of acrolein on Pt(111) and Pd(111) surfaces is investigated employing density functional theory calculations. The computed potential energy surfaces together with the analysis of reaction mechanisms demonstrate that steric effects are an important factor that governs chemoselectivity. The reactions at the C=O functionality require more space than the reactions at the C=C functionality. Therefore the formation of allyl alcohol is more favorable at low coverage, while the reduction of the C=C bond and the formation of propanal becomes kinetically more favorable at higher coverage. The elementary reaction steps are found to follow different reaction mechanisms, which are identified according to terminology typically used in organometallic catalysis. The transition state scaling (TSS) relationship is demonstrated and the origin of multiple TSS lines is linked to variation of an internal electronic structure of a carbon skeleton.*

The chemoselective hydrogenation of unsaturated aldehydes to saturated aldehydes and allylic alcohols has been extensively studied experimentally[1] and computationally[2] on metal surfaces. In particular, the chemo- and potentially also enantioselective reductions of α,β-unsaturated carbonyl compounds to the corresponding allylic alcohols are important processes in the pharmaceutical and fine chemical industry. In spite of the operational simplicity of the reduction on supported metal catalysts, the origin of the chemoselectivity (C=C vs. C=O reduction) with metals such as Pd and Pt remains largely unknown.[1a–j]

Experimentally, the simplest unsaturated aldehyde, acrolein, is reduced to propanal with over 98 % selectivity for C=C reduction with Pt catalysts.[1c–e] In contrast, hydrogenation of a more substituted aldehyde, such as prenal, is significantly less selective.[1f–h] Previous computational studies on hydrogenation of acrolein over Pt(111) propose that the reaction should indeed be selective for the C=O reduction, but the high desorption barrier of the allyl alcohol product controls the chemoselectivity and leads to isomerization and formation of propanal.[2b] However, experimental evidence does not appear to support the buildup of unsaturated alcohol on the Pt surface.[1i] Herein, we employ extensive density functional theory calculations and show that the discrepancy between experimental and computational studies disappears when 1) alternative mechanistic pathways are considered, 2) weaker adsorption sites are included in the analysis, and finally 3) steric effects are taken into account.

Typically, the barriers for repositioning the substrate on the surface, or transferring to an alternate binding mode, are considerably lower than the barriers for the key reaction steps.[3] According to the Curtin–Hammett principle,[4] these potentially equilibrating geometries should be easily accessible under the reaction conditions.[5] For this reason, we have attempted to carefully examine pathways originating from alternative binding modes. Second, when considering different possible elementary steps for the reaction pathways, we have attempted to correlate these mechanisms to the basic mechanism types of organometallic chemistry. The value of analyzing reaction pathways in this way becomes evident in the transition state scaling (TSS)[6] correlations with the reanalyzed reaction pathways, when the TSS correlations between transition state energies and adsorption energies are examined.

If the hypothesis of accumulation of allyl alcohol on Pt(111) holds, isomerization of allyl alcohol to propanal should take place under hydrogen pressure on the Pt surface. However, in our own hydrogenation experiments with allyl alcohol on Pt/C, 1-propanol was formed as the major product (> 95 %). In a control experiment without H_2 gas, allyl alcohol did not isomerize to propanal over 24 h reaction time.[7] These results do not support the notion that allyl alcohol should accumulate on the Pt(111).[2b]

The issue of chemoselectivity and the reaction mechanism were then addressed by density functional theory calculations.[8] The adsorption geometries and energies of acrolein (as *s-trans* conformer),[9] prenal, possible intermediates, and reaction products were first determined on Pd(111) and Pt(111) surfaces and are presented in detail in the Supporting Information. We considered several different adsorption geometries, as the most stable geometries may not necessarily lie on the major reaction pathway. Furthermore, transition state geometries and energies were determined for various different elementary steps. With this information at hand, we then investigated the reaction mechanisms with varying acrolein coverage and analyzed the impact of steric effects on the kinetically most favored reaction pathways and product selectivity. Experimental studies indicate that, partially hydrogenated or fragmented species are present on the surface under the reaction conditions.[1i,j,10]

These species bind strongly to the surface and block adsorption sites, thus disfavoring reaction pathways requiring access to several adjacent metal atoms. Such coverage effects

[*] S. Tuokko, Prof. Dr. P. M. Pihko, Dr. K. Honkala
Department of Chemistry, Nanoscience Center
University of Jyväskylä
P.O. Box 35, 40014, Jyväskylä (Finland)
E-mail: karoliina.honkala@jyu.fi

Supporting information for this article is available on the WWW under http://dx.doi.org/10.1002/anie.201507631.

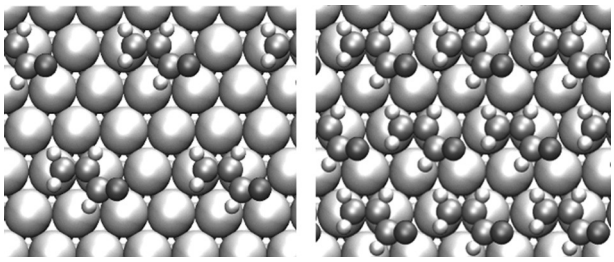

Figure 1. Acrolein adsorption geometries at 1/9 ML (left) and 1/4 ML (right) on a Pd(111) surface.

are in general steric in nature, and thus the precise chemical nature of the adsorbed species is less important.[1d,7,11]

On both studied metal surfaces, the adsorption geometries are similar: while the C=C bond lies parallel to the surface, the C=O bond is tilted away from the surface, see Figure 1. In the most stable adsorption geometry, acrolein (**1**) is bound via the C=C bond in the di-δ configuration **1*** (Figure 2) with the adsorption energy of −55 kJ mol^{-1} on Pd(111). When the coverage increases to 1/4 ML, the steric repulsion between acrolein molecules increases, leading to less exothermic adsorption energy, −31 kJ mol^{-1}, at the di-δ configuration.

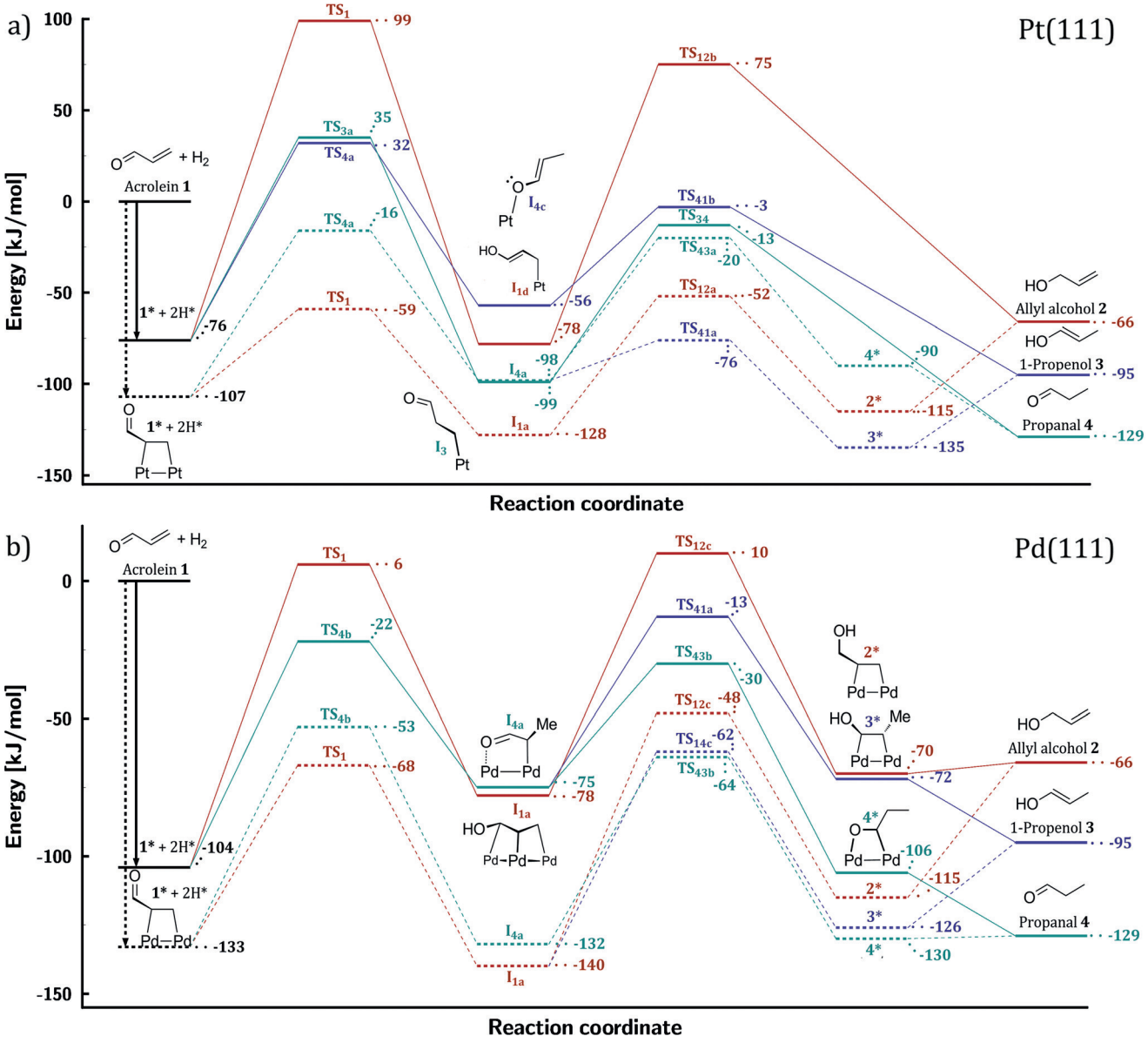

Figure 2. The potential energy surfaces for the key elementary steps in acrolein reduction a) on Pt(111) and b) on Pd(111) surfaces together with the key molecular structures. The integer numbers (most of them negative) refer to energy changes with respect to acrolein in gas-phase, while integers from 1–4 stand for acrolein and the possible product molecules. The adsorbed species are indicated by *. The short hand notations are as follows: TS stand for a transition state and I for an intermediate. The number subscripts refer to atoms in acrolein to which H is added. For example, subscript 12 refers to a case where H is first added to an oxygen and then to the carbonyl carbon. The letter in the subscript refers to a particular geometry among the possible optimized geometries shown in the Supporting Information. The solid line refers to the results at 1/3 (1/4) ML acrolein coverage on Pt (Pd) and the dashed line for 1/9 ML coverage.

On Pt(111), the adsorption energy of acrolein **1*** is −46 kJ mol^{-1} at 1/9 ML coverage, in agreement with previous calculations,[2b–e] and −5 kJ mol^{-1} at 1/3 ML coverage.

Among the three possible isomeric product molecules (allyl alcohol (**2**), 1-propenol (**3**) and propanal (**4**)), propanal is thermodynamically the most stable species in the gas phase by 35 kJ mol^{-1},[1i] while their relative stabilities on Pd(111) and Pt(111) differ (see Figure 2).

In order to identify the factors behind the experimentally observed chemoselectivity, the full potential energy surface (PES) for various partial hydrogenation pathways of acrolein (**1**) was computed. Figure 2 displays the PES for the kinetically most relevant pathways for different products on a Pt(111) surface at 1/9 and 1/3 ML coverage and on a Pd(111) surface at 1/9 and 1/4 ML coverage. The PES plots demonstrate that with increasing coverage the pathway for 1,2-reduction, that is, the formation of allyl alcohol (**2**), becomes less favorable on both metals.

To be more specific, on a Pt surface, the energy difference ($\Delta\Delta E^*$) between the highest transition state energies leading to allyl alcohol (**2**) or propanal (**4**) is 43 kJ mol^{-1} at 1/9 ML coverage, suggesting that the formation of allyl alcohol should dominate. In contrast, at the 1/3 ML coverage, the trend is reversed and the pathway leading to propanal (**4**) is favored with $\Delta\Delta E^* = 64$ kJ mol^{-1} (Figure 2).[12] Similar trends are observed on the Pd(111) surface, where the calculations do not solely predict that allyl alcohol (**2**) would be the major product even at low coverage (1/9 ML) since differences in transition state energies are within the typical error in DFT calculations. However, the energy differences between the allyl alcohol (**2**) and propanal (**4**) producing pathways increase upon increasing coverage, evolving from 5 kJ mol^{-1} to 32 kJ mol^{-1}.[13]

The most favorable first elementary steps on Pt(111) at 1/9 ML coverage are the reactions at the carbonyl oxygen with a barrier of 48 kJ mol^{-1} (**TS$_1$**) and at the β-carbon (**TS$_{4a}$**), with a barrier of 91 kJ mol^{-1}, in agreement with previous calculations.[2b–d] Although the barrier for the second elementary step on the allyl alcohol (**2**) pathway is somewhat higher (76 kJ mol^{-1}, **TS$_{12a}$**), the barrier of the first elementary step for the C=C reduction (**TS$_{4a}$**) is still higher, which further suggests that the formation of allyl alcohol (**2**) should be favored on Pt(111) at low coverage. However, these barrier heights are completely reversed to disfavor the formation of allyl alcohol (**2**) at 1/3 ML coverage as shown in Figure 2 a. On Pd(111), the kinetically most relevant first elementary step is the hydrogenation of β carbon (**TS$_{4b}$**), which has an activation energy of 82 kJ mol^{-1} at 1/4 ML coverage, while the barrier for the reaction at carbonyl oxygen (**TS$_1$**) is 28 kJ mol^{-1} higher (Figure 2 b).

On both surfaces, the substantial increase in the barrier height of carbonyl oxygen follows from the lack of free space on the surface and increased steric hindrance (Figure 1), which prevent the C=O functionality from turning down towards the surface. At 1/9 ML coverage, the C=O moiety can approach the surface without extra energy cost; thus it is easily accessible for a reaction with adsorbed hydrogen. Analysis of transition state geometries reveals that reactions at the C=O functionality necessarily require the involvement of an ensemble of three (possibly even four) metal atoms. The reactions at the C=C functionality are less space intensive and the size of the ensemble is on average two metal atoms. Our results nicely agree with the findings for 1-epoxy-3-butene on the (111) surfaces of Pt and Pd, which highlight the importance of coverage and adsorbate orientation for controlling selectivity.[14] Finally, we note that the steric effects also impact the product determining step. At 1/4 ML coverage, the first elementary step is now a product determining step, since the lowest barriers for the second elementary step lead to the formation of either propanal (**4**) or 1-propenol (**3**), which after desorption can isomerize to the aldehyde **4** via keto-enol tautomerism.[15]

To address the effect of alkyl substitution on an α,β-unsaturated aldehyde, the adsorption energies and geometries as well as key elementary reduction steps were studied with prenal, a β,β-dimethyl-substituted α,β-unsaturated aldehyde, on Pt(111) at 1/16 ML coverage.[7] The calculations show that the adsorption of prenal and its derivatives are weaker than acrolein analogs owing to the steric repulsion between methyl groups in a β carbon and the Pt(111) surface. For example, the adsorption energy of prenal is 21 kJ mol^{-1} weaker compared to acrolein. Therefore a building up of higher surface coverage of prenal, or the formation of partially hydrogenated species, is less probable with prenal than with acrolein and thus the impact of steric effects on the energetics of pathways is less significant. The PES (see Figure S10) unravels again that the reaction at carbonyl oxygen has the lowest barrier, among the possible first elementary steps. The lowest barrier for the second elementary step is the reduction of a β carbon, which is only 9 kJ mol^{-1} more favorable than the competing pathway and leads to enol, 3-methyl-1-butenol. However, the desorption barrier of enol is high (63 kJ mol^{-1}) compared to that of allylic alcohol (45 kJ mol^{-1}), therefore the computational results tentatively suggest that allylic alcohol is the first species to be observed in gas phase.[7]

In general, our results indicate that the increasing steric repulsions may result in significant changes in the conformation and binding geometry of the adsorbed substrate. These energy changes affect the entire reaction pathway: transition states accessible at low coverage may become strongly disfavored with increasing steric repulsion at high coverage, altering the selectivity and even the mechanism of the reaction.

Scheme 1 summarizes the major computationally identified pathways and mechanisms for the formation of allyl alcohol (**2**), 1-propenol (**3**) and propanal (**4**).[16] We use the terminology typically used for organometallic reaction mechanisms[17] (olefin insertion, protonation, reductive elimination and proton-coupled electron transfer (PCET)[18] to describe the mechanistic pathways. It should be noted that the analogy between mechanistic pathways in homogenous, homonuclear organometallics and heterogeneous metal surfaces cannot be exact, especially since a metal surface can easily act as either an electron source or electron sink—or even both, with different metal atoms donating and accepting electrons.[19]

The reduction of the C=C bond could take place via consecutive 4- and 3-addition steps (two formal reductive

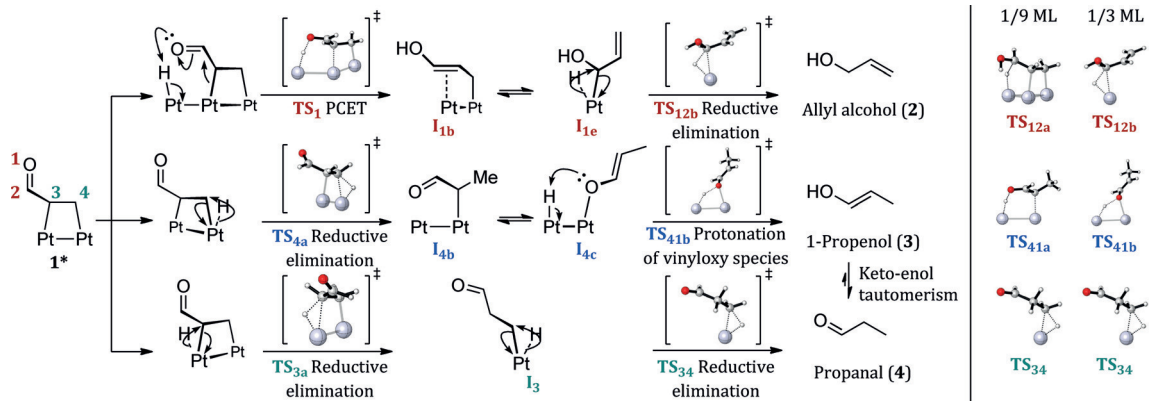

Scheme 1. Three mechanistic pathways for the formation of different products via PCET, reductive elimination, and protonation steps. The color coding is the same as in PES plots in Figure 2. On the right, the comparison of selected transition state geometries at 1/9 ML and 1/3 ML coverage.

elimination steps, where a C–M bond becomes a C–H bond, Scheme 1), producing propanal (**4**). Alternatively, consecutive 4- and 1-addition steps, that is, via reductive elimination and enol protonation steps (Scheme 1, middle), will give 1-propenol (**3**) which then rapidly tautomerizes to **4**. Additional pathways for the formation of **4** or **3** via other mechanisms, such as olefin insertion, have also been considered and computed (see the Supporting Information for details), but these pathways were energetically less favorable. The lowest identified energy pathway for the formation of allyl alcohol (**2**), takes place via consecutive 1- and 2-additions (PCET and reductive elimination steps).

Importantly, increasing the steric effects (i.e. coverage) on the metal strongly disfavors the 1- and 2-addition sequence that leads to allyl alcohol (**2**, Figure 2), resulting in increased selectivity for **4**. Visually, the difference between low (1/9 ML) and high (1/3 ML) coverage can be seen in the corresponding mechanisms for the second step (Scheme 1, right panel).

The final aspect we discuss is the TSS relationship, which was developed to link reaction transition state energies with adsorption energies. Similar to previous studies,[20] we find the universal TSS correlation for studied reductive steps of acrolein and prenal on Pd(111) and Pt(111) surfaces at different coverages (see Figure S12). Upon zooming into the universal TSS line, the existence of fine structure or noise is revealed. Typically, this deviation of points from the TSS line is identified to result from a local variation in adsorption geometries and differences in transition state bond lengths.[21] Herein, the fine structure appears to have a different origin. Figure 3 shows that we find separate and distinguishable TSS lines for each mechanism, which originate from a different internal electronic structure of a reacting species. Specifically, we find that the electronic structure of the bound species must be similar in order to two elementary steps to form a single TSS line.[22] For example, the internal electronic structure of the allyloxy and vinyloxy species differ, and thus they do not form one TSS line (see Figure S14). However, despite variations in adsorption geometry a single TSS line can be established.[7] Our results demonstrate that the previously derived extended TSS line for acrolein reduction on Pt-

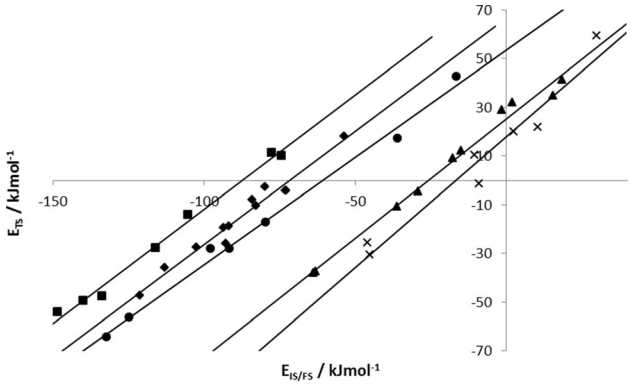

Figure 3. TSS relation for different mechanism: ■ olefin insertion (1,2-addition, $R^2 = 0.990$), ◆ reductive elimination (4,3-addition and 3,4-addition, $R^2 = 0.969$), ● PCET (1-addition, $R^2 = 0.993$), ▲ allyloxy protonation (2,1-addition, $R^2 = 0.989$), and × hydride addition (2-addition, $R^2 = 0.952$).

(111)[2d] is not necessary if the reaction mechanisms are carefully identified. The detailed mechanisms and electronic structures do matter in establishing the correlations.

In conclusion, the computed potential energy surface for partial reduction of acrolein on Pd(111) and Pt(111) demonstrates that steric effects are important for chemoselectivity. In this study, these steric effects were studied by increasing the substrate coverage on the metal surface. This is further supported with a careful analysis of mechanistic pathways, which highlight that reactions at the C=O functionality require more space than at the C=C functionality. The identified reaction mechanisms can be correlated and classified into the basic mechanisms in organometallic chemistry. This analysis helped us to establish TSS correlation lines between transition state energies and adsorption energies of initial/final states with good correlation. Depending on the internal electronic structure of the adsorbed substrate, different TSS lines are found even for mechanistically similar pathways. Similar calculations and analysis including the steric effects can potentially be important for other polyfunctional molecules to unravel the reasons behind chemoselectivity.

Acknowledgments

Support from the Graduate School of the Faculty of Science, University of Jyväskylä (to S.T.) and a grant from Tekes (2671/31/2013, to K.H. and P.M.P.) are gratefully acknowledged. We also acknowledge access to computational resources provided by the Finnish IT Center for Science (CSC).

Keywords: chemoselectivity · density functional theory · heterogeneous catalysis · reaction mechanism · surface chemistry

How to cite: *Angew. Chem. Int. Ed.* **2016**, *55*, 1670–1674
Angew. Chem. **2016**, *128*, 1702–1706

[1] a) P. Gallezot, D. Richard, *Catal. Rev. Sci. Eng.* **1998**, *40*, 81–126; b) P. Mäki-Arvela, J. Hájek, T. Salmi, D. Y. Murzin, *Appl. Catal. A* **2005**, *292*, 1–49; c) T. B. L. W. Marinelli, S. Nabuurs, V. Ponec, *J. Catal.* **1995**, *151*, 431–438; d) T. B. L. W. Marinelli, V. Ponec, *J. Catal.* **1995**, *156*, 51–59; e) V. Ponec, *Appl. Catal. A* **1997**, *149*, 27–48; f) P. Beccat, J. C. Bertolini, Y. Gauthier, J. Massardier, P. Ruiz, *J. Catal.* **1990**, *126*, 451–456; g) P. Claus, *Top. Catal.* **1998**, *5*, 51–62; h) T. Birchem, C.-M. Pradier, Y. Berthier, G. Cordier, *J. Catal.* **1994**, *146*, 503–510; i) C. J. Kliewer, M. Bieri, G. A. Somorjai, *J. Am. Chem. Soc.* **2009**, *131*, 9958–9966; j) J. C. de Jesús, F. Zaera, *Surf. Sci.* **1999**, *430*, 99–115; k) K. Brandt, M. E. Chiu, D. J. Watson, M. S. Tikhov, R. M. Lambert, *J. Am. Chem. Soc.* **2009**, *131*, 17286–17290; l) K. R. Kahsar, D. K. Schwartz, J. W. Medlin, *J. Am. Chem. Soc.* **2014**, *136*, 520–526; m) F. Zaera, *Chem. Rev.* **1995**, *95*, 2651–2693; n) K.-H. Dostert, C. P. O'Brien, F. Ivars-Barceló, S. Schauermann, H.-J. Freund, *J. Am. Chem. Soc.* **2015**, *137*, 13496–13502.

[2] a) J. W. Medlin, *ACS Catal.* **2011**, *1*, 1284–1297; b) D. Loffreda, F. Delbecq, F. Vigné, P. Sautet, *Angew. Chem. Int. Ed.* **2005**, *44*, 5279–5282; *Angew. Chem.* **2005**, *117*, 5413–5416; c) D. Loffreda, F. Delbecq, F. Vigné, P. Sautet, *J. Am. Chem. Soc.* **2006**, *128*, 1316–1323; d) D. Loffreda, F. Delbecq, F. Vigné, P. Sautet, *Angew. Chem. Int. Ed.* **2009**, *48*, 8978–8980; *Angew. Chem.* **2009**, *121*, 9140–9142; e) S. Laref, F. Delbec, D. Loffreda, *J. Catal.* **2009**, *265*, 35–42; f) K. H. Lim, A. B. Mohammad, I. V. Yudanov, K. M. Neyman, M. Bron, P. Claus, N. Rösch, *J. Phys. Chem. C* **2009**, *113*, 13231–13240; g) B. Yang, D. Wang, X.-Q. Gong, P. Hu, *Phys. Chem. Chem. Phys.* **2011**, *13*, 21146–21152; h) M. S. Ide, B. Hao, M. Neurock, R. J. Davis, *ACS Catal.* **2012**, *2*, 671–683; i) D. Loffreda, F. Delbecq, P. Sautet, *Chem. Phys. Lett.* **2005**, *405*, 434–439; j) D. Loffreda, Y. Jugnet, F. Delbecq, J. C. Bertolini, P. Sautet, *J. Phys. Chem. B* **2004**, *108*, 9085–9093.

[3] a) P. S. Cremer, X. Su, Y. R. Shen, G. A. Somorjai, *J. Am. Chem. Soc.* **1996**, *118*, 2942–2949; b) M. Neurock, R. A. van Santen, *J. Phys. Chem. B* **2000**, *104*, 11128–11145; c) A. M. H. Rasmussen, M. N. Groves, B. Hammer, *ACS Catal.* **2014**, *4*, 1182–1188; d) B. Yang, X.-Q. Gong, H.-F. Wang, X.-M. Cao, J. J. Rooney, P. Hu, *J. Am. Chem. Soc.* **2013**, *135*, 15244–15250.

[4] A. D. McNaught, A. Wilkinson in *IUPAC Compendium of Chemical Terminology*, 2nd ed. (the "Gold Book"), Blackwell Scientific Publications, Oxford, **1997**; XML on-line corrected version: http://goldbook.iupac.org (**2006**-), created by M. Nic, J. Jirat, B. Kosata, updates compiled by A. Jenkins.

[5] a) J. V. Barth, *Surf. Sci. Rep.* **2000**, *40*, 75–149; b) A. U. Nilekar, J. Greeley, M. Mavrikakis, *Angew. Chem. Int. Ed.* **2006**, *45*, 7046–7049; *Angew. Chem.* **2006**, *118*, 7204–7207.

[6] S. Wang, V. Petzold, V. Tripkovic, J. Kleis, J. G. Howalt, E. Skulason, E. M. Fernandez, B. Hvolbæ, K. G. Jones, A. Toftelund, H. Falsig, M. Bjorketun, F. Studt, F. Abild-Pedersen, J. Rossmeisel, J. K. Nørskov, T. Bligaard, *Phys. Chem. Chem. Phys.* **2011**, *13*, 20760–20765.

[7] For details, see the Supporting Information.

[8] a) J. Enkovaara, et al., *J. Phys.: Condens. Matter.* **2010**, *22*, 253202; b) for more details, see the Supporting Information.

[9] Using the *s-cis* conformer of acrolein as a reactant leads to the similar results and conclusions as presented in the Supporting Information.

[10] Substrates detected on the surface in the reaction conditions include: carbon monoxide, ethane, propene, ethylidyne and ketene; see Ref. [1i] and [1j].

[11] a) M. Neurock, V. Pallassana, R. A. van Santen, *J. Am. Chem. Soc.* **2000**, *122*, 1150–1153; b) F. Calaza, D. Stacchiola, M. Neurock, W. T. Tysoe, *J. Am. Chem. Soc.* **2010**, *132*, 2202–2207; c) S. T. Marshall, J. W. Medlin, *Surf. Sci. Rep.* **2011**, *66*, 173–184.

[12] Calculated as $\Delta(TS_1-TS_{4a})$ for 1/9 ML coverage and $\Delta(TS_1-TS_{3a})$ for 1/3 ML coverage).

[13] Calculated as the difference of the highest transition state energies $TS_{12c}-TS_{4b}$ for both coverages.

[14] a) A. S. Loh, S. W. Davis, J. W. Medlin, *J. Am. Chem. Soc.* **2008**, *130*, 5507–5514; b) S. T. Marshall, C. M. Horiuchi, W. Zhang, J. W. Medlin, *J. Phys. Chem. C* **2008**, *112*, 20406–20412; c) S. H. Pang, J. W. Medlin, *J. Phys. Chem. Lett.* **2015**, *6*, 1348–1356.

[15] The calculations were carried out with the RPBE functional but all the main results were also verified with the BEEF-vdW functional. The comparison of these results confirms that van der Waals interactions do not contribute to a reaction mechanism or chemoselectivity.

[16] For a discussion of alternative pathways, see the Supporting Information.

[17] J. F. Hartwig, *Organotransition Metal Chemistry: From Bonding to Catalysis*, University Science Books, Mill Valley, CA, **2010**.

[18] D. R. Weinberg, C. J. Gagliardi, J. F. Hull, C. F. Murphy, C. A. Kent, B. C. Westlake, A. Paul, D. H. Ess, D. G. McCafferty, T. J. Meyer, *Chem. Rev.* **2012**, *112*, 4016–4093.

[19] R. I. Masel, *Chemical Kinetics and Catalysis.* Wiley, New York, **2001**, chap. 14, p. 838.

[20] S. G. Wang, B. Temel, J. Shen, G. Jones, L. Grabow, F. Studt, T. Bligaard, F. Abild-Pedersen, C. H. Christensen, J. K. Nørskov, *Catal. Lett.* **2011**, *141*, 370–373.

[21] T. R. Munter, T. Bligaard, C. H. Christensen, J. K. Nørskov, *Phys. Chem. Chem. Phys.* **2008**, *10*, 5202–5206.

[22] a) E.-U. Würthwein, G. Lang, L. H. Schappele, H. Mayr, *J. Am. Chem. Soc.* **2002**, *124*, 4084–4092; b) H. Mayr, A. R. Ofial, *Angew. Chem. Int. Ed.* **2006**, *45*, 1844–1854; *Angew. Chem.* **2006**, *118*, 1876–1886.

Received: August 14, 2015
Revised: November 13, 2015
Published online: January 6, 2016

